ELSEVIER

February 1994

Optical Materials 3 (1994) 25–33

OPTICAL Materials

Excited state absorption and looping mechanism in Yb^{3+}-Tm^{3+}-Ho^{3+}-doped $Gd_3Ga_5O_{12}$ garnet

A. Brenier, L.C. Courrol, C. Pédrini, C. Madej, G. Boulon

Laboratoire de Physico-Chimie des Matériaux Luminescents, Unité de recherche associée au CNRS n°442, Université Claude Bernard-Lyon I, 43 Bd 11 Novembre 1918, 69622 Villeurbanne Cedex, France

Received 18 May 1993; revised manuscript received 9 September 1993

Abstract

Conversion of infrared laser light (near 753 nm) into green emission has been obtained in $Gd_3Ga_5O_{12}$:Yb:Tm:Ho by a two-step process: absorption from the fundamental states of the ions followed by a looping mechanism. The latter is composed by an absorption from the $^5I_7$(Ho) excited state and by a positive feedback process. A two-ion model to describe the dynamics is given and the gain and losses of the loop are evaluated.

1. Introduction

In a previous paper [1] we presented a study devoted to the sensitization of Ho^{3+} 2 μm laser emission by Yb^{3+}-Tm^{3+} ions in $Gd_3Ga_5O_{12}$ garnet. This system is attractive for laser diode pumping. We measured, with an integrating cavity, the up-conversion energy loss quantum yield when infrared pumping the Yb ion and we showed that in the triply doped crystal it is smaller than in the Yb-Ho doubly doped one. This might be due to the existence of efficient down-conversion mechanisms which bring the up-converted energy in the $^5S_2$–$^5F_4$(Ho) levels towards the 2 μm emitting level, the $^5I_7$ manifold. A positive feed-back process might result, increasing the population of the $^5I_7$ manifold. The purpose of this work is to discuss a candidate process. The excitation chosen is a continuous laser one near 753 nm and corresponding to the $^5I_7 \rightarrow {}^5S_2$–$^5F_4$(Ho) excited state absorption in such a way that a looping mechanism occurs. The result is the conversion of the infrared excitation into a green emission. If the gain of the loop is positive and greater than the losses a photon avalanche can occur. This phenomena is of particular interest in the case where absorption from the fundamental manifold is weak and has been studied more than ten years. More, up to now most of the studies had been devoted to singly doped matrices: Pr^{3+} [2–4], Sm^{3+} [5], Nd^{3+} [6–9], Tm^{3+} [10], Ni^{2+} [11]. The model that we give here concerns two ions: Ho^{3+} and Tm^{3+}, both having an active role. The Yb^{3+} ion does not play an active role at low temperature but may at room temperature. The model shows that a threshold for the avalanche exists and that its theoretical value depends of the absorption from the fundamental state: the larger is the absorption, the higher is the threshold. In our experiment the density of excitation remained below the threshold.

2. Experimental methods

The studied crystals were grown in our laboratory by the Czochralski method. The concentration $C(l)$ of one dopant in a sample cut at a distance l (along the axis of the crystal) from the origin $l=0$ of the

SSDI 0925-3467(94)E0036-B

crystal, and its coefficient of segregation k have been obtained by using the well known relations:

$$C(l)/C(0) = [1-g(l)]^{k-1},$$

$$C(0) = kC(\text{melt}), \quad (1)$$

where $g(l)$ is the crystallized fraction of the melt at point l. The ratio $C(l)/C(0)$ is deduced from the absorption spectra of the dopant. The coefficients of segregation of the Yb, Tm, Ho ions have each been found to be about 1.2. The concentrations of the dopants in the studied samples are gathered in Table 1.

The infrared excitation spectra were obtained with a cw tunable Ti:sapphire laser from Coherent (2 GHz resolution) pumped with a Coherent 300 argon ion laser. The laser beam was chopped at 10 Hz frequency and focused on the sample with a 5 cm focal length lens. The Ho green emission was detected with a Hamamatsu R1477 photomultiplier through a Jobin-Yvon H10D monochromator and the 2 μm Ho emission with a Judson InSb cell through an interference filter. Both detectors were coupled to a digital 9410 Lecroy oscilloscope. The samples were placed inside a liquid nitrogen cooled cryostat.

3. Excited state absorption

The laser excitation spectrum of the Ho green emission (near 540 nm, transition $^5S_2$–$^5F_4 \rightarrow {}^5I_8$) is shown in Fig. 1 at 300 and 77 K, in the doubly Yb(5%)–Ho(3%) doped sample (a) and in the triply Yb(5%)–Tm(5%)–Ho(0.5%) doped one (b) (a scheme of the Yb–Tm–Ho levels is given in Fig. 2). Because in this range of wavelengths (at least up to 762 nm) there is no *peak* of absorption from the Yb–

Table 1
Composition of $Gd_{3(1-x-y-z)}Yb_xTm_yHo_zGa_5O_{12}$ crystals.

x	y	z	Yb	Tm	Ho
(at.%)			(10^{20} ions/cm^3)		
5	0	0	7.0	0	0
0	5	0	0	7.9	0
5	5	0	8.5	8.8	0
5	0	0.5	8.0	0	0.74
5	0	3	8.6	0	4.6
5	5	0.5	7.7	8.9	0.76

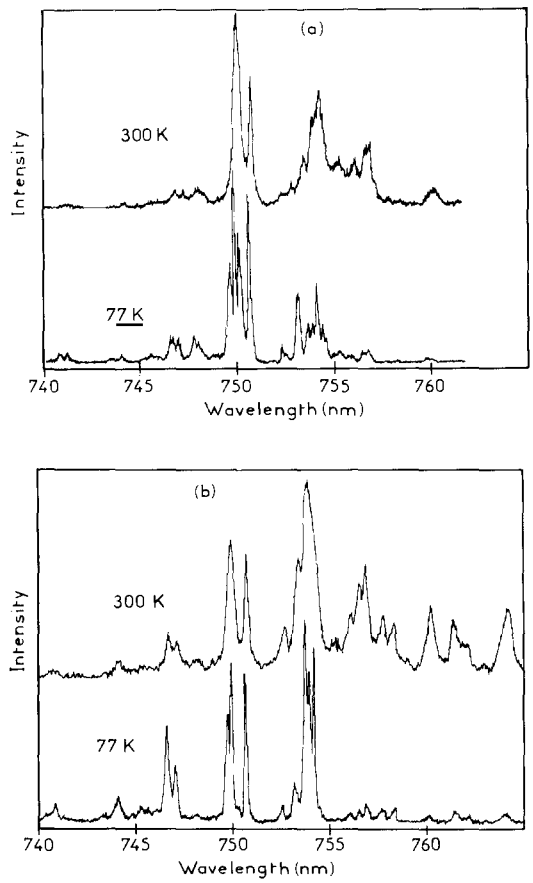

Fig. 1. Laser excitation spectra of the Ho green emission in the Yb(5%)–Ho(3%) doubly doped sample (a) and in the Yb(5%)–Tm(5%)–Ho(0.5%) triply doped sample (b).

Tm–Ho fundamental levels (see the absorption spectrum (curve 1) in Fig. 3) there is no difficulty to attribute the absorption of the laser beam by the $^5I_7 \rightarrow {}^5S_2$–$^5F_4$(Ho) excited state transition, the $^5I_7$ level being fed first by a structureless vibronic absorption from the fundamental states. More, the similarity between the excitation spectrum of Fig. 1b at 300 K and the absorption cross-section $\sigma_a(\lambda)$ of the $^5I_7 \rightarrow {}^5S_2$–$^5F_4$(Ho) transition represented in Fig. 4 is clear. This cross-section was deduced from McCumber relations connecting emission and absorption spectra [12]. The emission cross-section $\sigma_e(\omega)$ is related to the emission spectrum $f(\omega)$ at frequency ω:

$$f(\omega) = \sigma_e(\omega)\ (\omega n/2\pi c)^2, \quad (2)$$

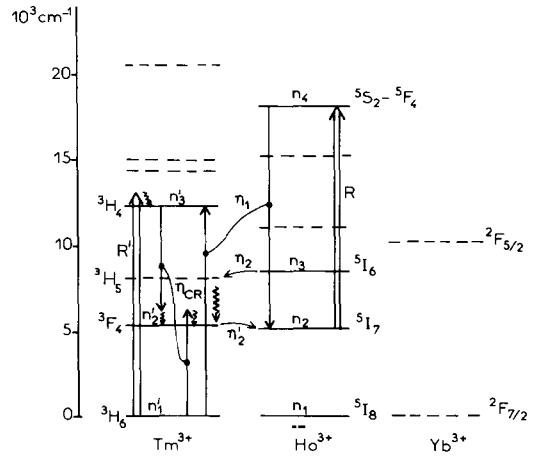

Fig. 2. Scheme of the energy levels and mechanisms involved in the model of Sect. 4. The dashed lines represent non considered levels.

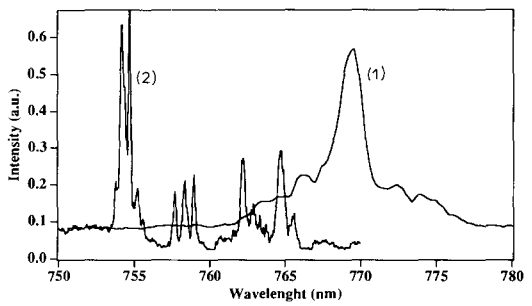

Fig. 3. Curve (1): Part of the absorption spectrum at 10 K of the Tm(5%) doped sample corresponding to the transition $^3H_6 \rightarrow {}^3H_4$. It is structureless up to 762 nm. Curve (2): Emission spectrum at 10 K corresponding to the $^5S_2$–$^5F_4 \rightarrow {}^5I_7$ transition in the Yb(5%)–Ho(3%) doped sample.

where $f(\omega)$ is normalized such that

$$1/\tau = 8\pi \int f(\omega)\, d\omega/2\pi . \qquad (3)$$

In Eq. (3) the radiative lifetime was taken from Ref. [13] and the emission spectrum $f(\omega)$ of the $^5S_2$–$^5F_4 \rightarrow {}^5I_7$ transition was experimentally recorded in the Yb–Ho doubly doped sample.

The $^5I_7 \rightarrow {}^5S_2$–$^5F_4$(Ho) excited-state absorption cross-section $\sigma_a(\omega)$ was then obtained knowing first the emission cross-section $\sigma_e(\omega)$:

$$\sigma_a = \sigma_e \exp(\hbar\omega/kT)(N_2/N_1)_e , \qquad (4)$$

$(N_2/N_1)_e$ is the ratio at thermal equilibrium of the two excited state populations involved in the transition. It is calculated by Boltzman law and requires the positions of the Stark sublevels. The Ho ions substitute the Gd ones and are in D_2 symmetry sites. In this case each $^{2S+1}L_J$ manifold of Ho^{3+} is split into $2J+1$ sublevels, labeled Γ_1, Γ_2, Γ_3, Γ_4 corresponding to the irreducible representations of the D_2 point group. Because neither electric nor magnetic dipole transitions are allowed between sublevels corresponding to the same irreducible representation [14] the positions of some of them cannot be found without crystal field calculation even with low temperature absorption and emission measurements. So Boltzman's law was applied using only the range of energy in which the Stark sublevels of a given manifold are distributed, the distribution being taken as a continuous one.

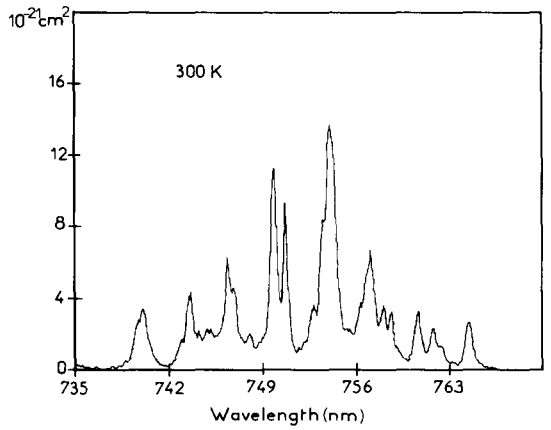

Fig. 4. Excited state absorption cross-section of the transition $^5I_7 \rightarrow {}^5S_2$–$^5F_4$(Ho).

We see from Fig. 4 that the excitated state absorption cross-section peak occurs at 753.9 nm and its value is 1.36×10^{-20} cm^2 (at 300 K). This value is of the same order of magnitude as the one obtained in YAG:Ho [15] and the range of the spectrum is the same. At 77 K, we see from Fig. 1b that the peak occurs at 753.74 nm.

The intensity $I(t)$ of the transmitted beam by the sample shows the time evolution of the excited state absorption. $I(t)$ is represented in Fig. 5a, the laser wavelength being at 753.74 nm, the sample the triply Yb–Tm–Ho one and the temperature 77 K. A time $t=0$, when the laser beam is turned on, there is only absorption from the fundamental states of the ions because the $^5I_7$(Ho) level is empty. Then the $^5I_7$(Ho)

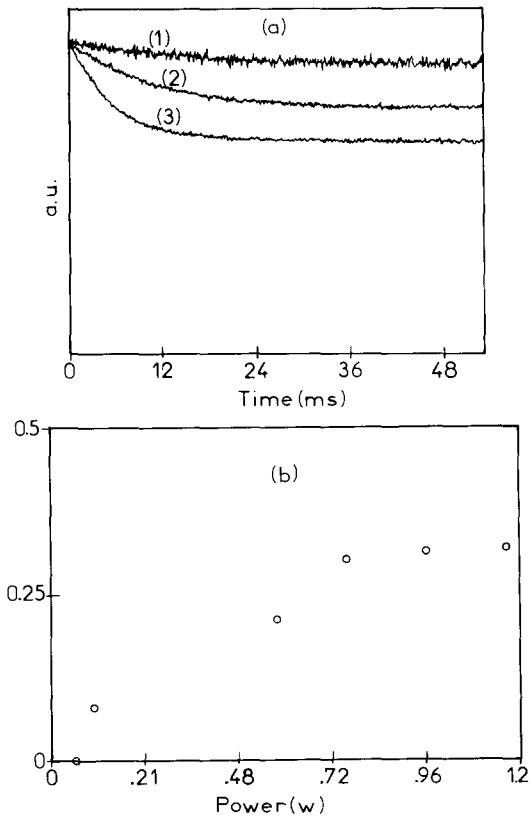

Fig. 5. (a) Time evolution of the flux of photons $I(t)$ of the transmitted laser beam at different incident power: (1) 0.113 W, (2) 0.580 W, (3) 1.17 W. (b) Ratio $[I(0)-I(\infty)]/I(0)$ versus incident power showing a saturation effect.

level fills and the transmitted intensity decreases. At long time the transmitted intensity $I(\infty)$ becomes constant and its value depends of the incident power. Fig. 5b shows the ratio $[I(0)-I(\infty)]/I(0)$ as a function of the incident power. The data above 0.72 W exhibit a saturation. At 1.17 W incident power the coefficient of absorption per unit length in the excited state $^5I_7$, calculated by the relation

$$[I(0)-I(\infty)]/I(0)=\exp(-kl)\,, \qquad (5)$$

where l is the length of the sample, has been found to be $k=1.1\ \mathrm{cm}^{-1}$.

4. Positive feed-back and looping mechanism

We have said that at first the laser excitation was absorbed by the Yb–Tm–Ho fundamental states (we shall identify which ones later), this absorption having a vibronic origin and being structureless. Then, directly or via transfer mechanisms, the $^5I_7$(Ho) level is fed. We want to examine now what happens to the $^5I_7$(Ho) population when the laser beam is simultaneously absorbed by the $^5I_7 \rightarrow {}^5S_2$–$^5F_4$(Ho) transition. The result is given by a laser excitation spectrum of the 2 μm Ho emission because this last one originates from the $^5I_7$ level and its intensity is proportional to the $^5I_7$ population. Such a spectrum is given in Fig. 6 (upper curve) at 77 K for the Yb(5%)–Tm(5%)–Ho(0.5%) sample. We can see that its peaks correspond exactly to the ones of the green emission laser excitation spectrum that we have reported again on the same Fig. 6 (lower curve). More, we can see that the first spectrum appears in *positive* values. This indicates that when a excitated state absorption occurs from the $^5I_7$ level it does not decrease its population but to the contrary it increases it. This fact proves that a positive feed-back process occurs. The origin of this process will be elucidated next.

The following study was done at 77 K. We recorded (Fig. 7) the decay time $n(t)$ of the Ho green emission after a direct pulsed excitation in the $^5S_2$–$^5F_4$(Ho) levels for the three samples: (1) Yb(5%)–Ho(0.5%); (2) Yb(5%)–Ho(3%); (3) Yb(5%)–Ho(0.5%)–Tm(5%). Because the decays are not exponential they have been fitted by the well-known Inokuti–Hirayama expression (dipole–dipole interaction) [16] and the quantum yield η of the energy transfers that they exhibit has been calculated with the formula

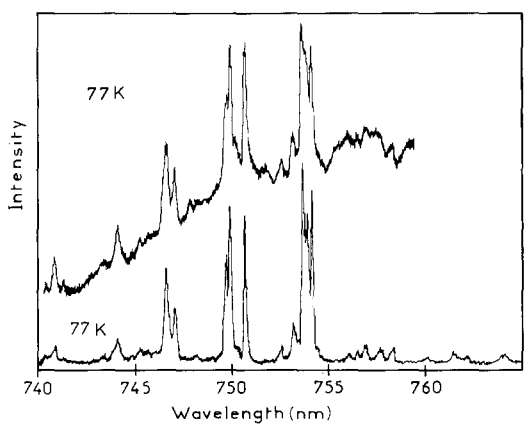

Fig. 6. Correlation between the 2 μm (upper curve) and the green (lower curve) Ho emission laser excitation spectra.

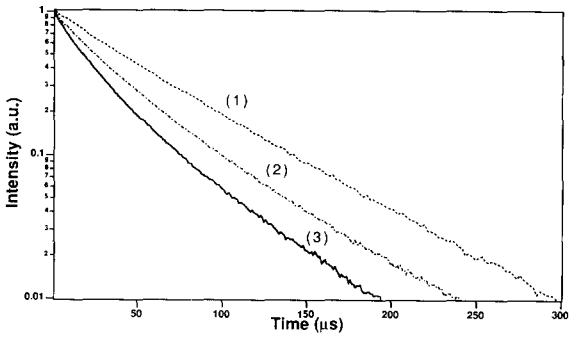

Fig. 7. Time evolution of the green Ho emission after a direct laser pulsed excitation in the $^5S_2$–$^5F_4$ levels at 77 K: (1) Yb(5%)–Ho(0.5%), (2) Yb(5%)–Ho(3%), (3) Yb(5%)–Ho(0.5%)–Tm(5%).

$$\eta = 1 - \int_0^\infty n(t)\,[\tau n(0)]\,\mathrm{d}t\,, \tag{6}$$

where $\tau = 63.2$ μs is the lifetime of the level given by the fit. For samples (1), (2), (3) the values of η are respectively 1.7%, 41%, 56.8%. The weak value of η for sample (1) (the decay is almost exponential) despite the presence of 5% Yb shows that transfers Ho→Yb, if any, can be neglected in all the samples. In fact inspection of results for sample (2) shows that a Ho–Ho cross-relaxation mechanism exists but we can neglect it in samples (1) and (2) because the Ho concentration is much weaker. Comparison of results for samples (1) and (3) proves that the Tm ions are responsible for the deexcitation of the $^5S_2$–$^5F_4$(Ho) levels. There are no Ho→Tm resonant transfers but the most nearly resonant one is

$$^5S_2 - {}^5F_4(\mathrm{Ho}),\ {}^3H_6(\mathrm{Tm}) \rightarrow {}^5I_7(\mathrm{Ho}),\ {}^3H_4(\mathrm{Tm})\,. \tag{7}$$

Its energy gap is only about 100 cm^{-1} (see Fig. 3). Morever, the back transfer of (7) has been claimed to be efficient in YAG:Tm:Ho [17] at room temperature despite of the unfavorable energy gap (it is negative).

We propose transfer (7) to be the first step of the feed-back process. The second one is the well known Tm–Tm cross-relaxation process:

$$^3H_4,\ {}^3H_6 \rightarrow {}^3H_5,\ {}^3F_4$$

(and then $^3H_5 \rightarrow {}^3F_4$ deexcitation) (8)

followed by the Tm→Ho transfer

$$^3F_4(\mathrm{Tm}),\ {}^5I_8(\mathrm{Ho}) \rightarrow {}^3H_6(\mathrm{Tm}),\ {}^5I_7(\mathrm{Ho})\,. \tag{9}$$

We note that at 77 K the back-transfer of (9) does not exist. (8) and (9) have been studied previously in $Gd_3Ga_5O_{12}$ [18,19].

Let us start with one ion in the $^5I_7$(Ho) level. If by excited state absorption the ion is sent into the $^5S_2$–$^5F_4$(Ho) levels, it will return to the $^5I_7$(Ho) level by the feed-back process with a certain efficiency and so a loop exists. But the number of $^5I_7$ ions found at the end of the loop is generally different from one and can be called the gain of the loop. We understand that if the gain is larger than the losses, the dynamics of the system will be qualitatively different from the case where it is smaller: in the first case we have a photon avalanche (as is proved in the appendix).

Now we want to describe the dynamic of the looping mechanism and find its gain in the Yb–Tm–Ho triply doped sample at 77 K after a continuous laser excitation at 753.74 nm. We propose the model represented in Fig. 2. The corresponding rate equations are

$$\begin{aligned}
\dot{n}_4 &= Rn_2 - n_4/\tau_4 - a_1 n_4 n_1'\,,\\
\dot{n}_3 &= -n_3/\tau_3 + b_3/\tau_4 n_4 - a_2 n_3 n_1'\,,\\
\dot{n}_2 &= -n_2/\tau_2 - Rn_2 + b_2/\tau_4 n_4 + a_1 n_4 n_1'\\
&\quad + (C_{\mathrm{Tm}}/C_{\mathrm{Ho}})a_2' n_2' n_1\,,\\
1 &= n_1 + n_2 + n_3 + n_4\,,\\
\dot{n}_3' &= -n_3'/\tau_3' + R' n_1' + (C_{\mathrm{Ho}}/C_{\mathrm{Tm}})a_1 n_4 n_1' - a_1' n_3' n_1'\,,\\
\dot{n}_2' &= -n_2'/\tau_2' + (1-b')/\tau_3' n_3' + 2a_1' n_3' n_1'\\
&\quad + (C_{\mathrm{Ho}}/C_{\mathrm{Tm}})a_2 n_3 n_1' - a_2' n_2' n_1\,,\\
1 &= n_1' + n_2' + n_3'\,,
\end{aligned} \tag{10}$$

with the initial conditions: $n_1 = n_1' = 1$ and $n_2 = n_3 = n_4 = n_2' = n_3' = 0$.

In Eqs. (10) the n_i, n_i' are fractions of populations, i.e. populations divided by the Ho or Tm concentrations, C_{Ho} or C_{Tm}, respectively.

In the model we haven taken into account the resonant transfer [1]

$$^5I_6(\mathrm{Ho}),\ {}^3H_6(\mathrm{Tm}) \rightarrow {}^5I_8(\mathrm{Ho}),\ {}^3H_5(\mathrm{Tm})\,, \tag{11}$$

and we have assumed that the absorption from the fundamental states was only due to Tm (The Ho con-

centration is 10 times weaker than the Tm one and the laser wavelength is close to the $^3H_4$(Tm) absorption peaks and far from the Yb ion ones.)

The coefficients a_i and a'_i describing the transfers have been calculated from the quantum yields η_i and η'_i of the transfers using relations such that for example

$$\eta_{CR} = a'_1/(1/\tau'_3 + a'_1)\,, \tag{12}$$

where η_{CR} was obtained by decay time analysis and (6). Eq. (12) means that in our model all the donor ions in a given transfer have the same transfer yield, independently of the acceptor distribution. Of course it is an approximation (for example the decays in Fig. 7 are not exponential) but this is the condition which allows us to use rate equations.

In (10) b_1, b_2, b_3 are respectively the branching ratios of the n_4 spontaneous deexcitation towards the n_1, n_2, n_3 levels and b' is the one of the n'_3 deexcitation towards n'_1. b_1, b_2, b' were calculated as radiative transitions using Judd–Offelt analysis and b_3 is $1-b_1-b_2$.

All the numerical values of the parameters involved in (10) are gathered in Table 2.

5. Result of fits and discussion

We have used system (10) to fit *simultaneously* the time evolution of the green Ho emission (curve 2, Fig. 8) and the ratio $I(t)/I(0)$, $I(t)$ being the intensity of the transmitted beam by the Yb–Tm–Ho doped sample. We had three fitting parameters: the absorption cross-section σ and σ' of the $^5I_7 \rightarrow {}^5S_2$–$^5F_4$(Ho) and $^3H_6 \rightarrow {}^3H_4$(vibronic)(Tm) transitions respectively and the area S of the laser beam focused on the sample. They are related to the yields R and R' by the relations

$$R = I\sigma/S \quad \text{and} \quad R' = I\sigma'/S\,, \tag{13}$$

where I is the flux of photons (photon/s) of the incident beam corresponding to an incident power of 1.17 W. Eqs. (13) shows that we did not take into account the variation of the flux of photons, I, inside the sample. Therefore, calculated populations have at a given time the same value at all points within the pumped region of the sample.

The experimental $I(t)/I(0)$ ratio was expressed using the relation

$$I(t)/I(0) = \exp\{-[C_{Ho} n_2 \sigma + C_{Tm}(n'_2 + n'_3)\sigma']l\}\,, \tag{14}$$

where $l = 0.34$ cm is the thickness of the sample. Eq. (14) can be established considering that

$$I(t) = I\exp[-(C_{Tm} n'_1 \sigma' + C_{Ho} n_2 \sigma)l]\,,$$
$$I(0) = I\exp(-C_{Tm}\sigma' l)\,, \tag{15}$$

where I is the flux of photons of the laser beam before the sample.

The result of the fits (circles in Fig. 8) are in agreement with the experimental data with the values of the fitting parameters:

$$\sigma = 1.73\times10^{-20}\,\text{cm}^2\,, \quad \sigma' = 6.16\times10^{-22}\,\text{cm}^2\,,$$
$$S = 5.44\times10^{-4}\,\text{cm}^2\,. \tag{16}$$

The value of σ at 77 K is larger than the one obtained at 300 K in Sect. 3 as expected.

Fig. 8 (curve 3) shows the transmission $T = I(t)/I$ of the sample. It visualizes at $t = 0$ the absorption from the Tm fundamental state. We find that it is not weak, as it is the case in the systems that exhibit a photon avalanche described in the literature. More, since this absorption is energy transferred to the Ho ions (with a quantum yield near 200%), the Ho ion pump rate is strong since the Ho concentration is about 10 times less than the Tm concentration. The consequences of this important fact are discussed below.

Next we calculate the gain of our loop. For simplicity, an equivalent three-level system described in the appendix and represented in Fig. A1 will be used. The role of our transfers (7), (8), (9) is played by the cross-relaxation mechanism in the three-level system

Table 2
Numerical values of the parameters involved in system (10). The lifetimes τ are given in ms.

τ_2	τ_3	τ_4	τ'_2	τ'_3	b_1	b_2	b'	η_1	η_2	η_{CR}	η'_2
9.4	0.550	0.063	17.1	0.722	0.177	0.042	0.327	56.8%	91.7%	96.7%	96%

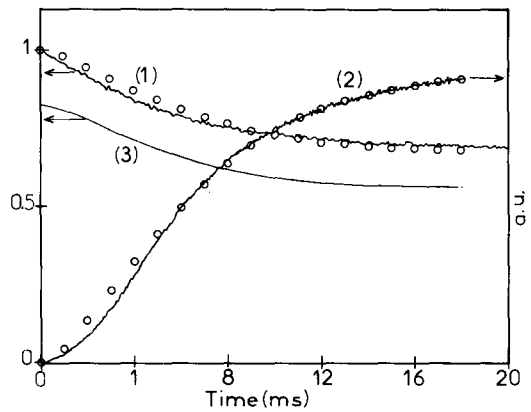

Fig. 8. Time evolution of: (1) $I(t)/I(0)$ ratio, (2) intensity of the Ho green emission, (3) transmission of the sample. The circles are the results of the fits.

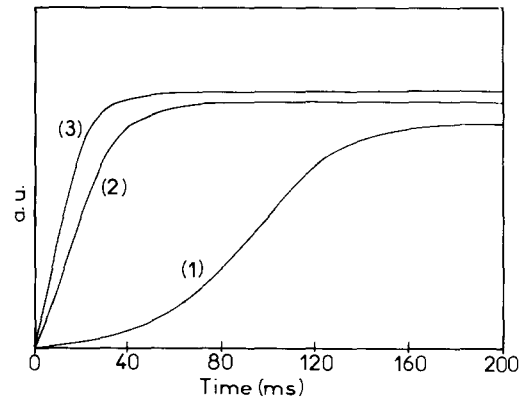

Fig. 9. Numerical simulation with system (10) of the time evolution of the green emission with different values of σ': (1) 0.05×10^{-22} cm^{-2}, threshold equal to gain; (2) 1.25×10^{-22} cm^{-2}, threshold smaller than gain; (3) 2.45×10^{-22} cm^{-2}, threshold higher than gain.

which leads to the following relation between quantum yields:

$$2H_{CR}=\eta_1+2\eta_1\eta_{CR}\eta'_2=1.622\,. \tag{17}$$

The absorption from the fundamental state is

$$R_1=R'(C_{Tm}/C_{Ho})2\eta_{CR}\eta'_2=21.7\,R'\,. \tag{18}$$

The excited state absorption is the same in the two systems: $R_2=R$. The branching ratio $1-B$ is such that

$$1-B=b_2+b_3\eta_2\eta'_2=0.729 \tag{19}$$

and then the quantum yield of the $3\rightarrow2$ deexcitation is

$$\eta=(1-B)(1-\eta_1)=0.315\,. \tag{20}$$

By using the formula (A.11) for the gain and the losses we find that the gain of the loop is 146.6 s^{-1} and the losses are 299.8 s^{-1}. So we find that the threshold of the photon avalanche is not reached in our system. This is due to the high value of the absorption from the fundamental Tm state. Nevertheless this high value associated with the positive feedback mechanism leads to an intense Ho green emission which would be smaller if we were in the conditions for avalanche. To prove this we did a numerical simulation of the time evolution of the green emission with system (10) (see Fig. 9) with three different values of σ', keeping the values of Table 2 for the other parameters and keeping σ and S given by (16). Then the gain of the loop remains 146.6 s^{-1}. One value of σ' is the one at which the threshold for avalanche is exactly the gain of the loop (curve 2) ($\sigma'=1.25\times10^{-22}$ cm^2, it was calculated with (18) introduced into (A.11)), one is such that the threshold is low enough to be smaller than the gain (curve 1), and the third is such that the threshold is higher than the gain (curve 3). Our system behaves as the latter case and Fig. 9 shows that the intensity of the green emission is larger at any time.

6. Conclusion

We have shown that a looping mechanism involving two species of ions occurs in $Gd_3Ga_5O_{12}$:Yb:Tm:Ho at low temperature. It is composed by an excited state absorption in the Ho ions followed by a positive feed-back process involving the Tm ions. Both looping mechanism and absorption of laser pump by the fundamental level of Tm ions have been included in a model to describe the conversion of the infrared pump beam into green emission. Despite the complexity of the system due to numerous energy levels our fits are in agreement with the experimental data. A simplified version of the model allowed us to calculate the gain and the loss of the looping mechanism from a theoretical expression, leading for the first time to the determination of the threshold for photon avalanche in the case of strong ground state pump transition. We show

that the threshold is an increasing function of the absorption from the ground state: the weaker the last one is, the easier it will be to obtain up-conversion via photon avalanche. But we show also that in our system the emission due to up-conversion is an increasing function of the absorption from the ground state so, a system that works below threshold can be more efficient than a system working above. We conclude that the systems that exhibit photon avalanche are not always the best ones to achieve up-conversion.

Acknowledgements

We are indebted to DRET and Region Rhône-Alpes for financial support of this research.

Appendix: threshold of stability and of photon avalanche

We consider here the simplest system that exhibits a looping mechanism, represented in Fig. A1. There is only one specie of ions. The loop is constituted by the excited state absorption (yield R_2) followed by a cross-relaxation process whose efficiency is H_{CR}. Despite of the fact that this system has been extensively modeled [4,8–10] no clear formula can be found in literature to express the threshold of photon avalanche whatever the pump rate in the ground state. This question is of special interest because the pump rate in the ground state can be modified by changing the concentration of one ion in the case of a two-ion system or by adding a second laser beam whose wavelength is in resonance with a line of the ground state absorption spectrum. The following equations

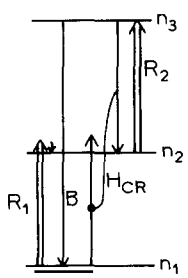

Fig. A.1. Scheme of the three level equivalent system.

describe the time evolution of the populations of the levels:

$$\dot{n}_2 = R_1 n_1 - r_2 n_2 - n_2/\tau_2 + n_3(1-B)/\tau_3 + 2\sigma n_1 n_3 , \tag{A.1}$$

$$\dot{n}_3 = R_2 n_2 - n_3/\tau_3 - \sigma n_1 n_3 , \tag{A.2}$$

$$1 = n_1 + n_2 + n_3 . \tag{A.3}$$

They are not linear because n_1 in the last terms of (A.1) and (A.2) is time dependent but this is not essential in early times. More, the nonlinearity is not essential in the sense that *it is not responsible for starting avalanche* but to the contrary it destroys it after a certain time. If we want to know if an avalanche occurs in a nonlinear system with a non small pump rate R_1 in the ground state, the best is to *test the instability of the associated linear system.* So, we shall learn much about the behaviour of the system by replacing $n_1(t)$ by a constant n_1 in the last term of (A.1) and (A.2). Eqs. (A.1) and (A.2) are now linear and their solutions approximate the ones of the initial equations at early times. Making their Laplace transforms we obtain the Laplace transform $\hat{n}_3(s)$ of $n_3(t)$ as

$$\hat{n}_3(s) = (R_2 R_1 n_1/s) \times [(s + r_1 + R_2 + 1/\tau_2)(s + 1/\tau_3 + \sigma n_1) - ((1-b)/\tau_3 + 2\sigma n_1 - R_1)R_2]^{-1} . \tag{A.4}$$

We can express σn_1 and the branching ratio $1-B$ of the $3\rightarrow 2$ deexcitation with the quantum yield H_{CR} of the cross-relaxation process and the quantum yield η of $3\rightarrow 2$ deexcitation:

$$H_{CR} = \sigma n_1/(1/\tau_3 + \sigma n_1) , \tag{A.6}$$

$$\eta = [(1-B)/\tau_3]/(1/\tau_3 + \sigma n_1) . \tag{A.7}$$

Then (A.4) becomes

$$\hat{n}_3(s) = \frac{R_1 R_2 n_1/s}{Q(s)} , \tag{A.8}$$

where $Q(s) = s^2 + Bs + C$ with

$$B = 1/\tau_2 + R_1 + R_2 + \frac{1}{\tau_3(1-H_{CR})}$$

(B is always positive)

$$C=\frac{1}{\tau_3(1-H_{CR})}$$
$$\times[1/\tau_2+R_1+R_1R_2\tau_3(1-H_{CR})$$
$$-R_2(2H_{CR}+\eta-1)]\,. \quad (A.9)$$

We know by using for (A.8) the standard methods to inverse the Laplace transforms that the time evolution $n_3(t)$ contains terms $\exp(\alpha t)$ where α are the roots of $Q(s)$. If at least the real part of one root is positive the system is unstable. Let us find the signs of the real part of the two roots.

(i) If the discriminant $\Delta=B^2-4C$ is negative (in this case C is always positive) the roots are complex and their real part is $-B/2$ which is always negative so the system is stable.

(ii) If the discriminant $\Delta=B^2-4C$ is positive the roots are reals and their product is C whose sign is the one of the term in brackets in (A.9): $1/\tau_2+R_1+R_1R_2\tau_3(1-H_{CR})-R_2(2H_{CR}+\eta-1)$. If this term is positive the two roots have the same sign and because their sum is negative $(-B)$ they are negative and the system is stable. If the term in brackets is negative:

$$R_2(2H_{CR}+\eta-1)>1/\tau_2+R_1+R_1R_2\tau_3(1-H_{CR})\,, \quad (A.10)$$

then the roots have opposite signs and one is positive: the system is unstable. The above discussion is resumed as

$$R_2(2H_{CR}+\eta-1)>1/\tau_2+R_1+R_1R_2\tau_3(1-H_{CR})$$
$$\leftrightarrow \text{system unstable}\,, \quad (A.11)$$

where the symbol $\leftrightarrow$ means "equivalent". Eq. (A.11) has a very simple physical interpretation. Its left side is the net gain of the loop: when an ion is removed (-1) from the n_2 level by laser beam (this occurs with a yield R_2) it is returned back by the cross-relaxation process with a quantum yield $2H_{CR}$ and by the $3\rightarrow2$ deexcitation with a quantum yield η. The right side of (A.11) describes the losses from the n_2: $1/\tau_2$ for the spontaneous deexcitation, R_1 and $R_1R_2\tau_3$ $(1-H_{CR})$ are losses of n_2 feeding by the laser pump due to accumulation of population into the n_2 and n_3 levels, respectively.

So when the net gain of the loop is larger than the losses the system is unstable and a photon avalanche occurs. In fact in this case the nonlinearity in system (A.1–A.3) due to the $n_1(t)$ time dependence comes into play and reduces the efficiency H_{CR} of the feedback mechanism ($n_1(t)$ is a decreasing function of t starting at 1). After a certain time the avalanche vanishes and populations reach stationary states. Nevertheless, two different regimes can exist, depending if condition (A.11) is fulfilled or not, and distinguishable qualitatively at early times (see the numerical simulation on Fig. 9). If the pump rate in the ground state R_1 is strong, (A.11) shows that it will be difficult to achieve avalanche and if achieved, it will be destroyed earlier by the nonlinearity and then hardly seen.

References

[1] A. Brenier, L.C. Courrol, C. Pédrini, C. Madej and G. Boulon, Phys. Rev. B, to be published.
[2] J.S. Chivian, W.E. Case and D.D. Eden, Appl. Phys. Lett. 35 (1979) 124.
[3] A.W. Kueny, W.E. Case and M.E. Koch, J. Opt. Soc. Am. B 6 (1989) 639.
[4] W.E. Case, M.E. Koch and A.W. Kueny, J. Lumin. 45 (1990) 351.
[5] N.J. Krasutsky, J. Appl. Phys. 54 (1983) 1261.
[6] N. Pelletier-Allard and R. Pelletier, Phys. Rev. B 36 (1987) 4425.
[7] N. Pelletier-Allard and R. Pelletier, J. Lumin. 46 (1990) 217.
[8] W. Length and R.M. Macfarlane, J. Lumin. 45 (1990) 346.
[9] M.F. Joubert, S. Guy and B. Jacquier, Phys. Rev. B 48 (1993) 10031.
[10] H. Ni and S.C. Rand, Optics Lett. 16 (1991) 1424.
[11] U. Oetliker, M.J. Riley, P.S. May and H.U. Gudel, J. Lumin. 53 (1992) 553.
[12] D.E. McCumber, Phys. Rev. 136 (1964) 954.
[13] Q. Wang, S. Zhang, S. Wu and X. Dong, J. Luminesc. 40&41 (1988) 181.
[14] J.B. Gruber, M.E. Hills, M. Seltzer, S.B. Stevens, C.A. Morrison, G.A. Turner and M.R. Kokta, J. Appl. Phys. 69 (1991) 8183.
[15] R.R. Petrin, M.G. Jani and R.C. Powell, Opt. Mater. 1 (1992) 111.
[16] M. Inokuti and F. Hirayama, J. Chem. Phys. 43 (1965) 1978.
[17] J.K. Tyminski, D.M. Franich and M. Kokta, J. Appl. Phys. 65 (1989) 3181.
[18] A. Brenier, C. Madej, C. Pédrini and G. Boulon, J. Phys.: Condens. Matter 3 (1991) 203.
[19] A. Brenier, G. Boulon, C. Madej, C. Pédrini and L. Lou, J. Lumin. 54 (1993) 271.